Chapter 10
Reconstruction of Femur Bone from DICOM Files and FEA on Fractured Human Femur Bone with PEEK Thermoplastic Prosthetic Plate Implantation

S. Kirthana and Mohammed Khaja Nizamuddin

Abstract The longest and strongest bone in the human body is the femur bone also known as the thigh bone supports the maximum weight of the body under loading conditions. Fracture of bones is one of the common issues in the present medical world. One of the methods to treat bone fractures is using prosthetic implants. There are different biomaterials that are used to make these prosthetic plates like metals, polymers, composites, and ceramics. The purpose of this work is to develop the femur bone model from DICOM files and analyze the fractured human femur shaft with PEEK thermoplastic prosthetic plate implant by FEA in static loading conditions. Results are compared with the other biomaterials like SS316L, alumina, and titanium to prove PEEK is also a suitable material for femur shaft fracture prosthetic plate implantation. The femur model is developed using 3D Slicer and Blender softwares. Analysis is done in ANSYS workbench 18.1.

Keywords Femur bone · DICOM files · PEEK · FEA · Prosthetic plate

10.1 Introduction

Fractures in femur bone are caused due to a large force, impact loads, accidents, fall from high altitudes, and disease in the bone. Classifications based on the severity of the fracture are stress fracture, severe impact fracture, partial fracture, and completely displaced fracture. One of the methods to treat bone fractures is using prosthetic implants. The types of prosthetic plates from early stages to the present day of implantation surgeries are compression plate (CP), dynamic compression

---

S. Kirthana (✉) · M. K. Nizamuddin
Department of Mechanical Engineering, Vasavi College of Engineering, Hyderabad 500031, India
e-mail: kirthana6831@gmail.com

M. K. Nizamuddin
e-mail: nizammohdk@gmail.com

C. Li et al. (eds.), *Advances in Engineering Design and Simulation*,
Lecture Notes on Multidisciplinary Industrial Engineering,
https://doi.org/10.1007/978-981-13-8468-4_10

plate (DCP), limited-contact dynamic compression plate (LC-DCP), point contact fixator (PC-Fix), less invasive stabilization system (LISS), locking compression plate (LCP), and precontoured LCP.

10.1.1 Different Materials Available for Manufacturing Prosthetic Plates

There are different biomaterials that are used to make these prosthetic plates like metals, polymers, composites, and ceramics. Stainless steel is mostly used in orthopaedic implants for temporary fixation plates where the plates are removed after the healing process is completed. Otherwise, it leads to allergy and toxic reactions in the body. Titanium alloys are the most usable implantation material as it has extensive mechanical properties, resistance to corrosion, resistance to fatigue corrosion, and low density. It was considered as the better material in implantation when compared with stainless steel. The examples of polymers and composites are polymethyl methacrylate (PMMA), poly lactic acid (PLA), poly glycolic acid (PGA). Alumina and hydroxyapatite (HA) come under the category of bioceramics. But these materials cannot be used directly as implants due to its low mechanical strength and low fracture toughness. But these materials can be used in the form of coatings and mixed ratios with other biomaterials.

The present work can be divided into two main categories. One is the reconstruction of bone from DICOM files and the second one is to do Finite element analysis fractured human femur bone with PEEK thermoplastic prosthetic plate implantation.

10.2 Reconstruction of the Femur Bone from DICOM Images

To develop the 3D models of bones or tissues, CT or MRI data is to be collected. CT or MRI data is saved in the form of DICOM files is used in CAD software to develop the models.

10.2.1 Reconstruction of Bone Using 3D Slicer

The collected DICOM files with the slice thickness of 0.6 mm were imported into this software. By enabling the volume rendering feature, we can observe the visualization of the files on the Slicer window in four views, i.e., axial view, three-dimensional view, sagittal view, and coronal view as shown in Fig. 10.1. A preset selection of CT bones was selected, and it can be observed that in the three-dimensional view, only

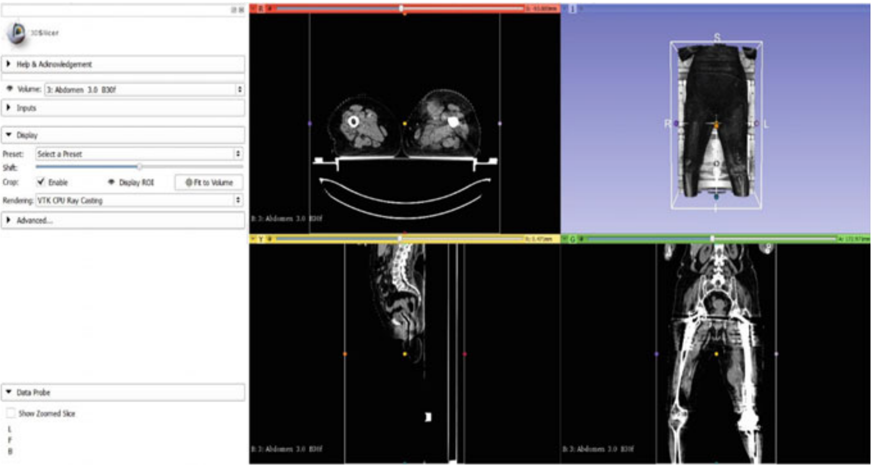

Volume: 3: Abdomen 3.0 B30f

Preset: Select a Preset

Shift:

Crop: ✓ Enable Display ROI Fit to Volume

Rendering: VTK CPU Ray Casting

☐ Show Zoomed Slice

Fig. 10.1 3D Slicer window showing four views

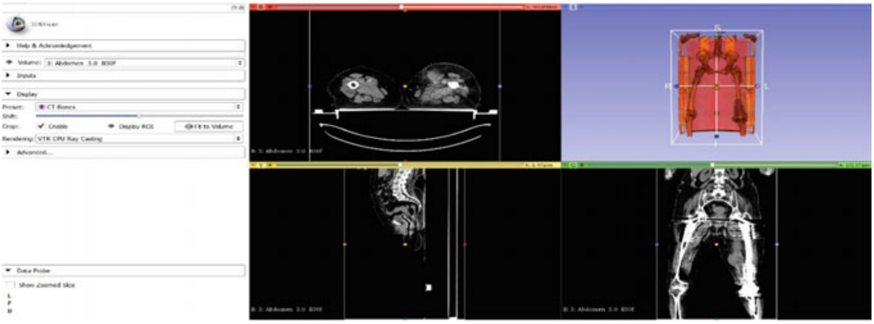

Volume: 3: Abdomen 3.0 B30f

Preset: CT-Bones

Shift:

Crop: ✓ Enable Display ROI Fit to Volume

Rendering: VTK CPU Ray Casting

☐ Show Zoomed Slice

Fig. 10.2 Preset selection

bones were visualized removing all the other unwanted material which is shown in Fig. 10.2.

After this, cropping was done by using the crop volume module. Here the cropping was done to get the right femur bone of the image. The cropped new volume is shown in Fig. 10.3.

From the obtained CAD model, it was observed that the model is with a lot of obstructions, irregularities, and discontinuities as it is already gone for a prosthesis with implantations. So to obtain the best model without any errors, the paint effect was used in the editor module. After using the paint effects, the best 3D cad model of the right femur is as shown in Fig. 10.4 [1, 2]. This obtained model was saved in STL file format as to import the model into the blender. The obtained model was with some errors, and the surface achieved was rough. To remove this, a software called Blender was used.

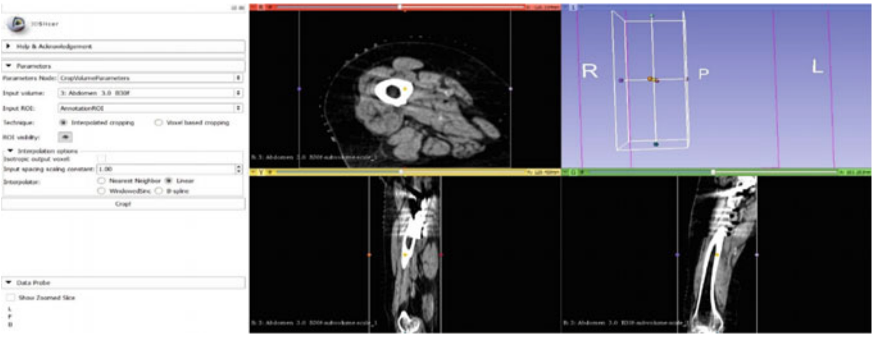

Parameters Node: CropVolumeParameters
Input volume: 3: Abdomen 3.0 B30f
Input ROI: AnnotationROI
Technique: ● Interpolated cropping ○ Voxel based cropping
Isotropic output voxel: ☐
Input spacing scaling constant: 1.00
Interpolator: ○ Nearest Neighbor ● Linear ○ WindowedSinc ○ B-spline
☐ Show Zoomed Slice

Fig. 10.3 Cropped volume

Fig. 10.4 Showing 3D CAD model of the right femur after using paint effect

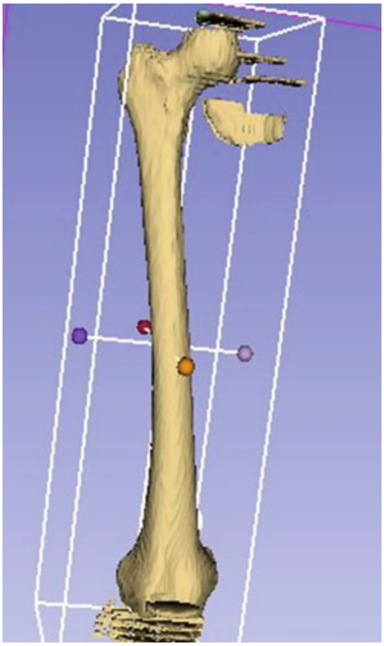

10.2.2 *Finishing the Femur Model Using Blender*

The obtained model from 3D Slicer was imported into Blender to remove the discontinuous shapes and errors and to obtain a good surface finish which is shown in Fig. 10.5 from the selection mode; the continuous and inverted links were selected by vertex selection, and the inverted links were deleted to obtain an error-free femur bone without any obstructions which are shown in Fig. 10.6a, b.

After applying the smoothening option from object modifiers, the final 3D CAD model of the femur with the good surface finish is shown in Fig. 10.6c.

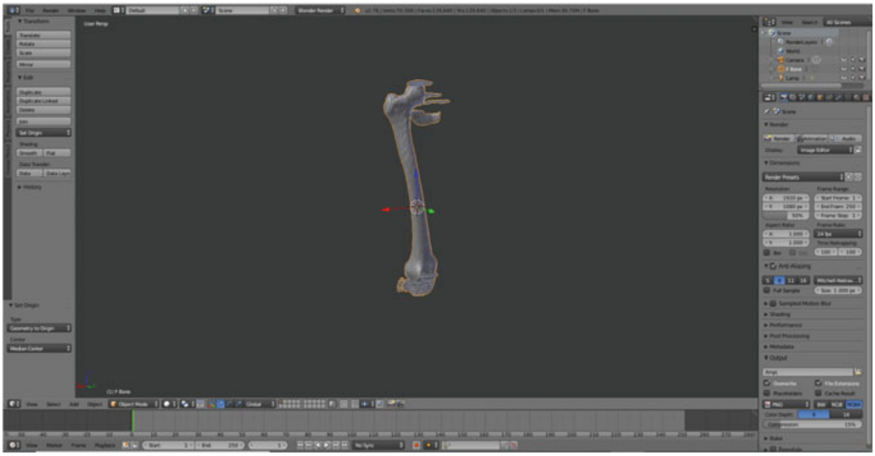

Fig. 10.5 Blender window with imported STL file of the right femur bone

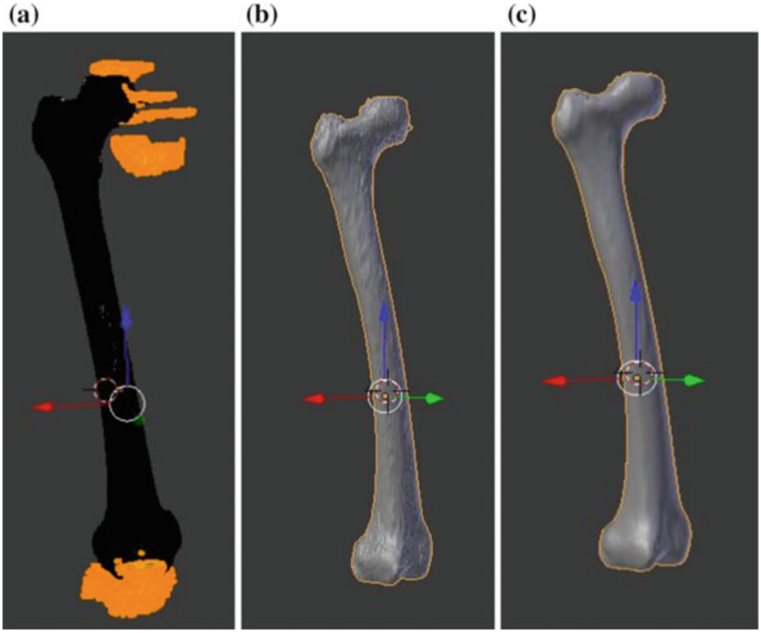

Fig. 10.6 Showing **a** inverted links **b** obtained model without errors **c** final 3D CAD model of the right femur with the good surface finish

Fig. 10.7 Fracture on femur shaft

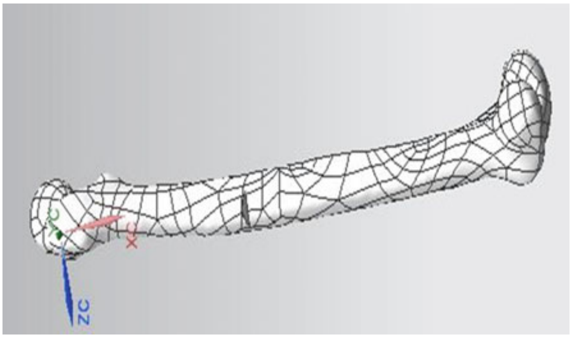

10.2.3 *Initiation of Fracture on Femur Bone*

Partial fracture was initiated for further study on analysis of fractured femur bone [3]. The fracture was generated in NX by removing the part material from the shaft of femur bone as shown in Fig. 10.7

10.3 Fractured Femur Bone Analysis

The fractured femur bone was inserted into the static structural module and the material properties of femur bone were assigned from Refs. [4, 5].

10.3.1 *Meshing*

Meshing of the fractured femur bone was done with element type triangular and element size of 5 mm.

10.3.2 *Boundary Conditions*

The lower part of the femur bone was fixed, and two forces on the upper part of the femur were assigned [6, 4].

Force 1: 750N, 150, 0 and Force 2: −150N, −50N, 0

Force 1 is the total body weight of the person which is acting downward when the person is standing, and force 2 is the reaction force which is acting in the opposite direction as shown in the Fig. 10.8.

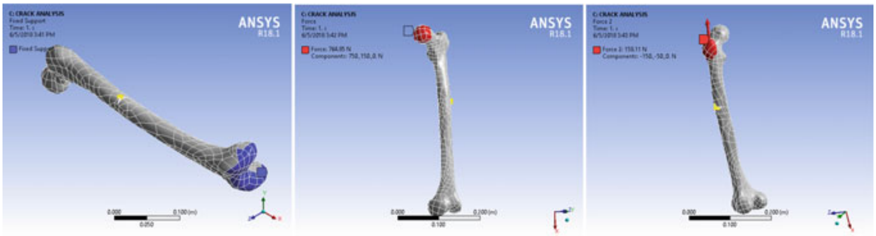

Fig. 10.8 Boundary conditions

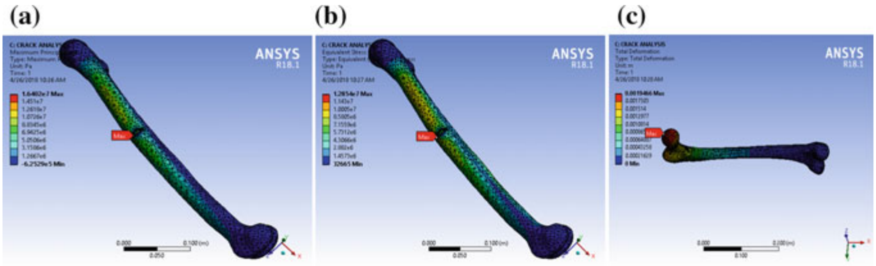

Fig. 10.9 Fractured bone **a** maximum principal stress **b** equivalent stress **c** total deformation

10.3.3 Results of Fractured Bone Analysis

A static structural analysis is carried out, and it was noted that the maximum stresses are acting on the shaft at the initiation of fracture for the boundary conditions that are considered and the total deformation was seen maximum on the head of the femur bone. The results are as shown below Fig. 10.9.

10.4 Assembly for Fractured Bone and Prosthetic Plate

In this work, the prosthetic plate of LCP type is modeled [7] and assembly is done in NX 11.0 assembly module as shown in Fig. 10.10. The meshed assembly of prosthetic plate and femur bone has 29,155 nodes and 16,030 elements. Bonded contact option in ANSYS was used to make sure that plate is in surface contact with the fractured bone.

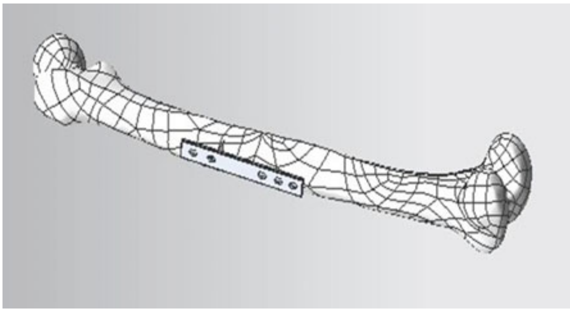

Fig. 10.10 Assembly of femur and prosthetic plate

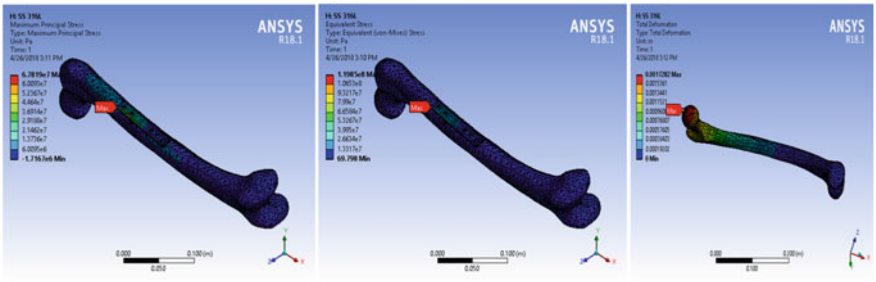

Fig. 10.11 Maximum principal stress, equivalent stress, and total deformation of fractured bone with SS316L plate

10.5 Assembly Analysis

Edge size meshing was generated at the crack by using the same mesh sizing as of fractured bone, and the boundary conditions are kept the same as of fractured bone. Analysis of the assembly was carried out by changing the material properties of prosthetic plates, from Refs. [8–11]. The results of stresses and deformation of prosthetic plate materials SS316L, alumina, titanium, and PEEK are as shown in Figs. 10.11, 10.12, 10.13 and 10.14. The results of maximum principal stress, equivalent stress, and total deformation are consolidated in Table 10.1.

10.5.1 Analysis Results of Fractured Bone with SS316L Prosthetic Plate

See Fig. 10.11.

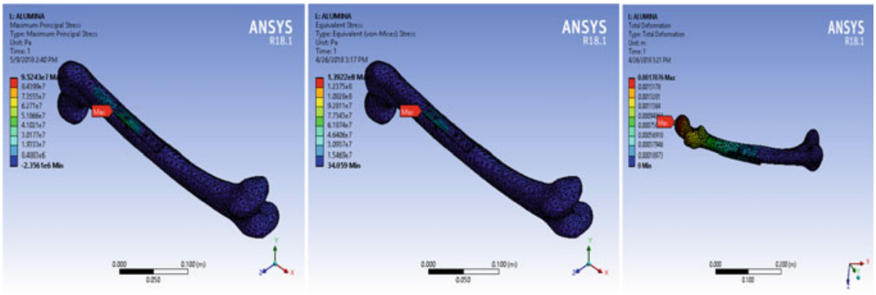

Fig. 10.12 Maximum principal stress, equivalent stress, total deformation of fractured bone with alumina plate

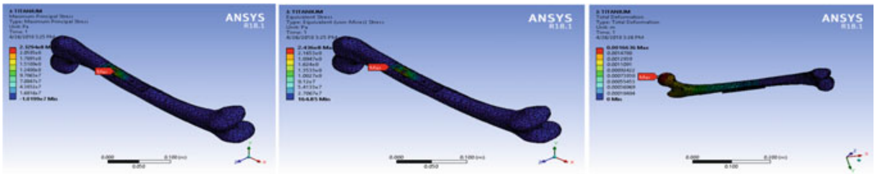

Fig. 10.13 Maximum principal stress, equivalent stress, and total deformation of fractured bone with titanium plate

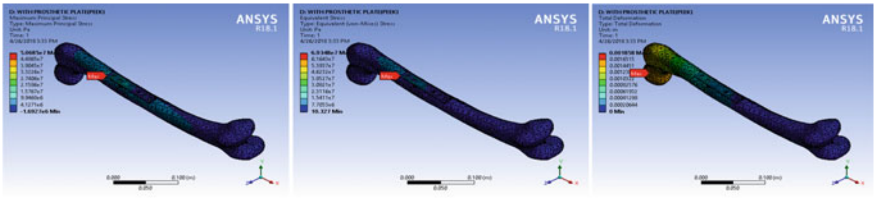

Fig. 10.14 Maximum principal stress, equivalent stress, and total deformation of fractured bone with PEEK plate

Table 10.1 Equivalent stress, maximum principle stress and total deformation of fractured bone and fractured bone with Prosthetic plates of different materials

	Equivalent stress (Pa)	Max principle stress (Pa)	Total deformation (m)
Fractured bone	1.2854e7	1.6402e7	0.0019466
Fractured bone with SS316L plate	1.1985e8	6.7819e7	0.0017282
Fractured bone with alumina plate	1.322e8	9.5243e7	0.0017076
Fractured bone with titanium plate	2.436e8	2.3294e8	0.0016636
Fractured bone with PEEK plate	6.9348e7	5.0685e7	0.001858

10.6 Analysis Results of Fractured Bone with Alumina Prosthetic Plate

See Fig. 10.12.

10.6.1 Analysis Results of a Fractured Bone with Titanium Prosthetic Plate

See Fig. 10.13.

10.6.2 Analysis Results of a Fractured Bone with PEEK Prosthetic Plate

See Fig. 10.14.

10.7 Results and Discussions

It was observed that the stresses are increased, and the deformations are reduced. The maximum stresses were acting on the plate which means that the bone was not taking the load. The decrease in the deformations means that the load-bearing capacity was increased by the plates which are affixed to the bone. The obtained maximum stresses and deformations are tabulated as shown in Table 6.1.

10.8 Conclusions and Future Scope

10.8.1 Conclusions

1. Femur bone was reconstructed successfully by using 3D Slicer and Blender softwares from DICOM files or CT scan data.
2. From the results, it was concluded that the stresses were increased and were acting on the plate, taking the maximum load.
3. It was concluded that deformations were decreased and so that the healing can be obtained with less time duration.
4. It was concluded that the titanium material plate fixation was best suitable material as the values of equivalent stress, maximum principal stress, and total defor-

mation are 2.436e8 Pa, 2.3294e8 Pa, and 0.0016636 m, respectively, showing the best results from other biometals.

5. PEEK can be concluded as compatible materials as the values of equivalent stress, maximum principal stress, and deformations are 6.9348e7 Pa, 5.0685e7 Pa, and 0.001858 m, respectively, and were in approximate range with the other biomaterials.

10.8.2 Future Scope

Fibers and other composite materials can be used as prosthetic plates in future which should be tested clinically [12].

Acknowledgements The authors would like to thank management and Department of mechanical engineering of Vasavi College of engineering for providing resources in successful completion of the project.
The authors would like to thank Dr. Shirish Chandra Gampa, MBBS, MDRT, Radiation Oncologist, KIMS Hospitals, Hyderabad, who helped to complete the project by providing the necessary files.

References

1. Baradeswaran, A., Joshua Selvakumar, L., Padma Priya, R.: Reconstruction of images into 3D models using CAD techniques. Euro. J. Appl. Eng. Sci. Res. **3**, 1–8 (2014)
2. Velazquez, E.R., Parmar, C., Jermoumi, M., Mak, R.H., Van Baardwijk, A., Fennessy, F.M., Lewis, J.H., De Ruysscher, D., Kikinis, R., Lambin, P., Aerts, H.J.: Volumetric CT-based segmentation of NSCLC using 3D-Slicer. Sci. Rep. **18**(3), 3529 (2013)
3. Reddy, M.V.K., Ganesh, B.K.C., Bharathi, K.C.K., ChittiBabu, P.: Use of finite element analysis to predict type of bone fractures and fracture risks in Femur due to Osteoporosis. J. Osteopor Phys. Act **4**(180), 2 (2016)
4. Dhanopia, A., Bhargava, M.: Finite element analysis of human fractured femur bone implantation with PMMA thermoplastic prosthetic plate. Procedia Eng. **173**, 1658–1665 (2017)
5. Chiu, W.K., Ong, W.H., Russ, M., Fitzgerald, M.: Simulated vibrational analysis of internally fixated femur to monitor healing at various fracture angles. Procedia Eng. **188**, 408–414 (2017)
6. Parashar, S.K., Sharma, J.K.: A review on application of finite element modelling in bone biomechanics. Perspect. Sci. **8**, 696–698 (2016)
7. Igna, C., Schuszler, L.: Current concepts of internal plate fixation of fractures. Bulletin UASVM, Veterinary Medicine **67**(2), 118–124 (2010). ISSN1843-5270
8. Deokar, N.D., Thakur, A.G.: Design development and analysis of femur bone by using rapid prototyping. IJEDR (2016). ISSN: 2321-9939
9. Malekani, J., Schmutz, B., Gu, Y., Schuetz, M., Yarlagadda, P.: Orthopedic bone plates: evolution in Structure, Implementation technique and biomaterial. GSTF J. Eng. Technol. (JET) **1**(1) (2017)
10. Nag, S., Banerjee, R.: Fundamentals of medical implant materials. ASM handbook **23**, 6–17 (2012)

11. Roeder, R.K., Conrad, T.L.: B.S. Bioactive polyaryletherketone composites. PEEK Biomaterials Handbook (2012). https://doi.org/10.1016/b978-1-4377-4463-7.10011-9
12. Basafa, E., Armiger, R.S., Kutzer, M.D., Belkoff, S.M., Mears, S.C., Armand, M.: Patient-specific finite element modeling for femoral bone augmentation. Med. Eng. Phys. **35**, 860–865 (2013)